

Stroboscopic nonlinear dynamics: a time-independent theoretical framework

Yuhui Zhuang^{1†}, Jiaxin Li^{1†}, Haidong Li¹, Siyu Li¹, Xiaobin Peng¹, Juan Wu², Jiameng Zhang¹, Mingjing Fan¹, Yi Hu^{1*}, and Jingjun Xu^{1**}

¹*Key Laboratory of Weak-Light Nonlinear Photonics, Ministry of Education, School of Physics, Nankai University, Tianjin 300071, China*

²*Pengcheng Laboratory, Shenzhen 518052, China*

[†]These authors contribute equally to this work.

^{*}e-mail: yihu@nankai.edu.cn, ^{**}jjxu@nankai.edu.cn

Abstract: Recent experiments have demonstrated the ability to manipulate nonlinear interactions via time modulation, giving rise to the so-called stroboscopic nonlinearity. To date, however, this phenomenon has not been subjected to a rigorous theoretical analysis. In this work, we elucidate the physical mechanism underlying stroboscopic nonlinear dynamics and establish an effective time-independent model under suitable modulation conditions. The proposed model almost exactly reproduces the full time-dependent dynamics in the quasi-steady state and significantly outperforms empirical descriptions used previously. Our results provide a clear physical picture of stroboscopic nonlinear dynamics and establish a general framework for engineering nonlinear interactions through temporal modulation.

1. Introduction

Time modulation provides a powerful tool for manipulating physical systems across diverse fields. By introducing time-dependent parameters, such as forces, potentials, couplings, or material properties, one can endow a system with novel characteristics that are not accessible in its static counterpart. For instance, time modulation can stabilize otherwise unstable states [1], induce parametric instability [2], break time-reversal symmetry [3], open momentum gaps [4], and lead to spontaneous breaking of time-translation symmetry [5]. Owing to these captivating functionalities, time modulation has been extensively applied in both classical and quantum regimes, giving rise to a variety of intriguing phenomena [6-20], which hold great promise for the development of innovative technologies.

Quite recently, time modulation has been further extended to engineer optical nonlinearity. Self-focusing and -defocusing nonlinearities, two opposite effects commonly seen in various materials, are tailored to occur stroboscopically. Such a setting, established in a photorefractive crystal, enables the interplay between self-focusing and -defocusing dynamics, yielding the nonreciprocal light-light interactions that violate the action-reaction principle [21]. This type of nonreciprocity, distinct from that based on time-reversal symmetry breaking, brings about novel and interesting phenomena, such as optical predator-prey dynamics [22] and unusual impulse-momentum relationships [23]. Although an empirical model, synthesized without incorporating time dependence, has been used to describe the stroboscopic nonlinearity and the associated experimental observations, the underlying physics and a complete theoretical framework remain lacking. In particular, it is still unclear how time modulation controls the form of nonlinear interaction and why a model independent of time has the potential to fit experimental realities.

In this work, we rigorously derive a time-independent model to describe the stroboscopic nonlinear dynamics. Starting from the band-transport model that governs the light-matter interactions in photorefractive crystals, we show that the stroboscopic dynamics eventually reach a quasi-steady state, provided that the stroboscopic period is much shorter than the crystal's dielectric time constant. During the quasi-steady evolution, the stroboscopic dynamics

can be approximately described by a time-independent model, where the two inverted nonlinear processes occurring in alternating time intervals effectively coexist simultaneously. Notably, the form of the derived nonlinearity has never been reported before in materials without time modulations. This approximate model shows excellent agreement with the full time-dependent model in capturing stroboscopic nonlinear dynamics and significantly outperforms empirical approaches. Our results elucidate rigorously the physical mechanism underlying the stroboscopic nonlinear dynamics and demonstrate the potential to engineer optical nonlinearities unattainable in static systems.

2. Theory

We start with the following equation that is derived from the well-known band-transport model in a photorefractive crystal [24-26]:

$$\frac{\partial}{\partial x} \left(\frac{\partial E(x, z, t)}{\partial t} + Q(x, z, t) E(x, z, t) \right) = 0, \quad (1)$$

where E is the space electric field, and $Q = \frac{1}{\tau_d} (1 + |u|^2)$ with u being an optical field and τ_d

being dielectric time constant. This time constant is governed by the crystal properties and dark illumination conditions, which are typically controlled by applying a background light source to the crystal. In general, τ_d ranges from milliseconds to tens of hours [27, 28]. Without loss of generality, we adopt $\tau_d = 50$ s in this work. Here, we only consider a single transverse direction (i.e., the x -axis), leaving the more complex scenario of two transverse dimensions for future investigation. From Eq. (1), one can readily obtain that the term $\frac{\partial E(x, z, t)}{\partial t} + Q(x, z, t) E(x, z, t)$ is x -independent. In the areas far away from the optical field (generally having a finite scale), corresponding to a condition of $u = 0$, the space electric field should be equal to the applied electric field denoted as $E_{ext}(t)$, which is formulated as:

$$\frac{\partial E}{\partial t} + QE = \left(\frac{\partial}{\partial t} + \frac{1}{\tau_d} \right) \lim_{x \rightarrow \pm\infty} E = \left(\frac{\partial}{\partial t} + \frac{1}{\tau_d} \right) E_{ext}. \quad (2)$$

With initial conditions of $E(x, z, t < 0) = 0$ and $E_{ext}(t = 0) = E_0$ (where E_0 is a constant, representing the initially applied external electric field), one can obtain the spatiotemporal evolution of the space electric field in the crystal by solving Eq. (2):

$$E(x, z, t) = \left\{ \int_0^t \left[\left(\frac{\partial}{\partial t'} + \frac{1}{\tau_d} \right) E_{ext}(t') \right] e^{\int_0^{t'} Q(x, z, t'') dt''} dt' + E_0 \right\} e^{-\int_0^t Q(x, z, t') dt'}. \quad (3)$$

To realize stroboscopic nonlinear dynamics, the applied electric field is adopted as square waves [Fig. 1(a)], which have a form of:

$$E_{ext}(t) = \begin{cases} E_+, & t \in \left(0, \frac{T}{2} \right] + (n-1)T \\ E_-, & t \in \left(\frac{T}{2}, T \right] + (n-1)T \end{cases}, \quad (4)$$

where $n = 1, 2, \dots$ and $E_+ = -E_- = E_0$. Meanwhile, the optical field is set to consist of two stroboscopic beams: during the time of E_+ and E_- , the optical field is denoted as $\varphi_+(x, z, t)$

and $\varphi_-(x, z, t)$, respectively [Fig. 1(a)]. Therefore, the term $Q(x, z, t)$ in each half of the period has the following form:

$$\begin{cases} Q_+(x, z, t) = \frac{1}{\tau_d} \left(1 + |\varphi_+(x, z, t)|^2 \right), & t \in \left(0, \frac{T}{2} \right] + (n-1)T \\ Q_-(x, z, t) = \frac{1}{\tau_d} \left(1 + |\varphi_-(x, z, t)|^2 \right), & t \in \left(\frac{T}{2}, T \right] + (n-1)T \end{cases}. \quad (5)$$

Equations (3-5) determine the space electric field, which in turn modulates the propagation of the two stroboscopic beams (here set to be extraordinarily polarized) through the Pockels effect:

$$i \frac{\partial \varphi_+(x, z, t)}{\partial z} = -\frac{1}{2n_0 k_0} \nabla_{\perp}^2 \varphi_+(x, z, t) - k_0 \Delta n(x, z, t) \varphi_+(x, z, t), \quad (6-1)$$

$$i \frac{\partial \varphi_-(x, z, t)}{\partial z} = -\frac{1}{2n_0 k_0} \nabla_{\perp}^2 \varphi_-(x, z, t) - k_0 \Delta n(x, z, t) \varphi_-(x, z, t), \quad (6-2)$$

$$\Delta n(x, z, t) = -\frac{1}{2} n_0^3 r_{33} E(x, z, t), \quad (6-3)$$

where k_0 is the wave vector in vacuum, n_0 is the unperturbed refractive index of the crystal, Δn is a light-induced refractive index change, and r_{33} is an electro-optic coefficient.

At the input (i.e., $z = 0$), the light intensity distribution $|\varphi_+(x, 0, t)|^2$ and $|\varphi_-(x, 0, t)|^2$ remain time-invariant, and so do the terms $Q_+(x, 0, t)$ and $Q_-(x, 0, t)$. In this framework, the space electric field can be obtained through calculating Eqs. (3-5). It is a summation of the applied electric field (i.e., E_{ext}) and a space charge field (denoted as E_{sc}), in which the latter has the following form in each half period over the interval $(N-1)T$ to NT (N is an integer):

$$\begin{aligned} E_{sc,+} = & \frac{E_0}{\tau_d Q_+} \left(1 - e^{-Q_+(t-(N-1)T)} \right) + \left(e^{-Q_+(t-(N-1)T)} - 1 \right) E_0 \\ & + E_0 \frac{1 - \tau_d Q_+}{\tau_d Q_+} \left(1 - e^{-Q_+ \frac{T}{2}} \right) \frac{1 - e^{-\frac{-(Q_+ + Q_-)T}{2}(N-1)}}{1 - e^{-\frac{-(Q_+ + Q_-)T}{2}}} e^{-\frac{Q_- T}{2}} e^{-Q_+(t-(N-1)T)} \end{aligned} \quad (7-1)$$

$$-E_0 \frac{1 - \tau_d Q_-}{\tau_d Q_-} \left(1 - e^{-Q_- \frac{T}{2}} \right) \frac{1 - e^{-\frac{-(Q_+ + Q_-)T}{2}(N-1)}}{1 - e^{-\frac{-(Q_+ + Q_-)T}{2}}} e^{-Q_+(t-(N-1)T)}, \quad t \in \left(NT - T, NT - \frac{1}{2}T \right],$$

$$\begin{aligned} E_{sc,-} = & -\frac{E_0}{\tau_d Q_-} \left(1 - e^{-Q_-(t - \frac{N-1}{2}T)} \right) - E_0 \left(e^{-Q_-(t - \frac{N-1}{2}T)} - 1 \right) \\ & + E_0 \frac{1 - \tau_d Q_+}{\tau_d Q_+} \left(1 - e^{-Q_+ \frac{T}{2}} \right) \frac{1 - e^{-\frac{-(Q_+ + Q_-)T}{2}N}}{1 - e^{-\frac{-(Q_+ + Q_-)T}{2}}} e^{-\frac{Q_- T}{2}} e^{-Q_-(t - \frac{N-1}{2}T)} \end{aligned} \quad (7-2)$$

$$-E_0 \frac{1 - \tau_d Q_-}{\tau_d Q_-} \left(1 - e^{-Q_- \frac{T}{2}} \right) \frac{1 - e^{-\frac{-(Q_+ + Q_-)T}{2}(N-1)}}{1 - e^{-\frac{-(Q_+ + Q_-)T}{2}}} e^{-Q_+ \frac{T}{2}} e^{-Q_-(t - \frac{N-1}{2}T)}, \quad t \in \left(NT - \frac{1}{2}T, NT \right].$$

The first two terms in Eqs. (7-1) and (7-2) describe the establishment of the space charge field during the last cycle, while the 3rd and 4th terms, decaying exponentially with time, account for the space charge field accumulated before the last cycle.

The time evolution described by Eq. (7) is illustrated by a typical example, where we set $\varphi_+ = 3e^{-x^2/w^2}$ and $\varphi_- = e^{-x^2/w^2}$ ($w = 12\mu\text{m}$) at $z = 0$ and choose the stroboscopic period as $T = 1$ s. Figure 1(b) plots the evolution of the space charge field. Here only the region of $x < 0\mu\text{m}$ is shown considering the inversion symmetry about $x = 0$. The space charge field builds up from zero and eventually reaches a steady state. These dynamics are further verified by the result presented in Fig. 1(c), which is obtained by directly simulating Eq. (2). More details are shown in Fig. 1(d) where the dynamics at $x = 0\mu\text{m}$ are plotted. During the evolution, the space charge field also undergoes small oscillations due to the applied square wave electric field; consequently, the final state corresponds to a quasi-steady state.

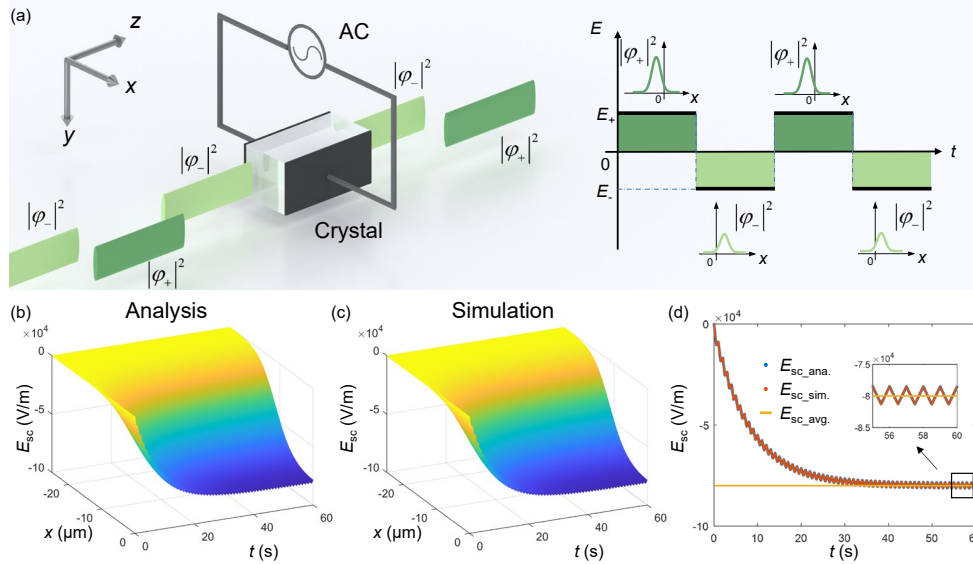


Fig. 1. (a) Schematic setup for realizing stroboscopic nonlinear dynamics: two stroboscopic optical fields (i.e., φ_{\pm}) are launched during positive or negative electric field that is externally applied to a photorefractive crystal (see the inset). (b, c) Evolution of the space charge field calculated by Eq. (7) (b) and simulated by Eq. (2) (c). (d) shows the dynamics of (b, c) at $x = 0$: red and blue dots correspond to (b) and (c), respectively, while the yellow solid line denotes the averaged value in the quasi-steady state.

For the propagation cross-section at $z = z_0$ ($z_0 > 0$), the refractive index change for $z < z_0$ varies much with time when the system has not reached a quasi-steady state, and so do the light distributions $\varphi_{\pm}(x, z_0, t)$. This time-dependent feature makes it impossible to analytically derive the space charge field at $z = z_0$ using the approach deriving Eq. (7). However, once a quasi-steady state is built, presumably at $t = t_0$, the light distributions $\varphi_{\pm}(x, z_0, t)$ can be approximately regarded as unchanged with time. Thus, the time-evolving space charge field for $t > t_0$ can be calculated; its form is similar to Eq. (7), except that the time variable needs to be replaced with $t' = t - t_0$ and a term including the space charge field accumulated in the period of $0 < t < t_0$ should be added, i.e., $E_{sc}(x, z_0, t_0) e^{-\frac{T}{2}(N-1)} e^{-\varphi_+(t'-(N-1)T)}$ and $E_{sc}(x, z_0, t_0) e^{-\frac{T}{2}(N-1)} e^{-\varphi_+\frac{T}{2}} e^{-\varphi_-\frac{T}{2}(N-\frac{1}{2})T}$ for Eq. (7-1) and Eq. (7-2), respectively. The additional term will eventually vanish when sufficient time elapses (i.e., $N \gg 1$), such that the

time evolution of the space charge field can still be described by Eq. (7). In general, more time is needed to build the quasi-steady state for a longer crystal. Besides, the building time is also determined by the initial distribution of the injected beams. In what follows, we compare the evolution of the space charge field by employing two input conditions with a slight difference. The first involves the injection of two stroboscopic Gaussian beams that are spatially overlapped at the input [Figs. 2(a, b)]; the second is identical, except that a small spacing is introduced between the two beams [Figs. 2(c, d)]. At the input, the building time is nearly the same for both cases, but at the output, it is longer for the latter, indicating that more complex input beam profiles tend to require more time to reach a quasi-steady state.

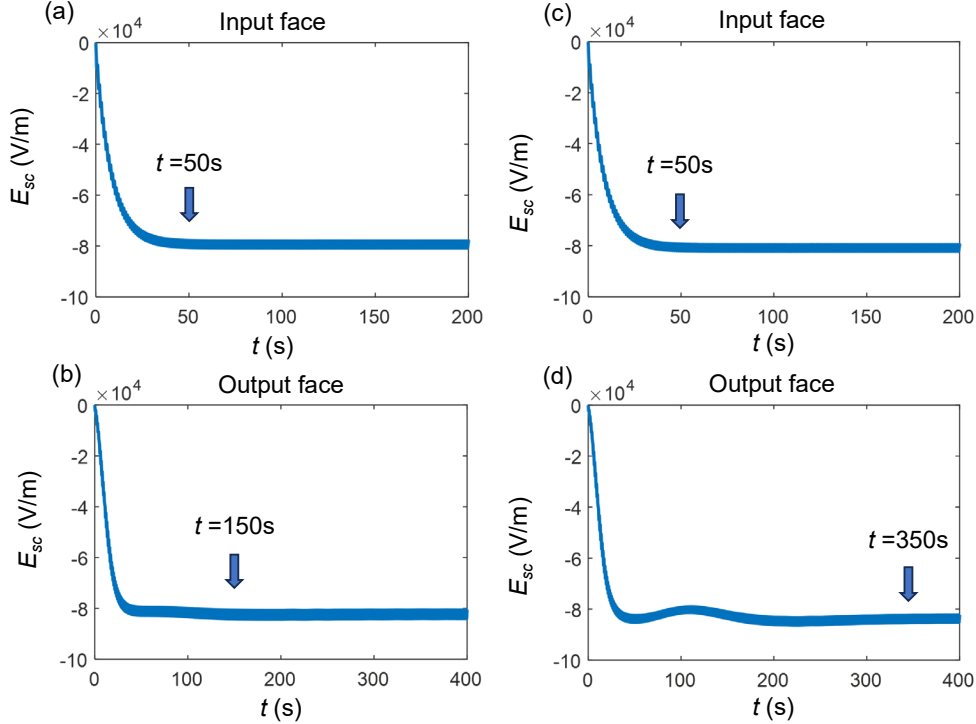


Fig. 2. Evolution of the space charge field (at $x = 0$) at the input (a, c) and output (b, d) by injecting two Gaussian beams with exact overlapping (a, b) or a small spacing (c, d). The arrows mark the time when a quasi-steady state is built.

For the quasi-steady state, the terms in Eq. (7) have the following approximation:

$$\frac{1-e^{-\frac{Q_+ T}{2}}}{1-e^{-\frac{(Q_+ + Q_-) T}{2}}} \approx \frac{Q_+}{Q_+ + Q_-}, \quad \frac{1-e^{-\frac{Q_- T}{2}}}{1-e^{-\frac{(Q_+ + Q_-) T}{2}}} \approx \frac{Q_-}{Q_+ + Q_-}, \quad 1-e^{-\frac{(Q_+ + Q_-) T}{2} N} \approx 1, \quad e^{-\frac{Q_+ T}{2}} \approx 1, \quad \text{and}$$

$$e^{-\frac{Q_-}{2} \left(t - \left(N - \frac{1}{2} \right) T \right)} \approx 1.$$

These derivations are obtained by using $N \gg 1$ (corresponding to sufficiently long time) and $(Q_+ + Q_-) \frac{T}{2} \ll 1$ (satisfied considering the stroboscopic period is quite small relative to τ_d). Then the space charge field described by Eq. (7) is approximated as:

$$E_{sc} = -\frac{|\varphi_+|^2}{2 + |\varphi_+|^2 + |\varphi_-|^2} E_0 + \frac{|\varphi_-|^2}{2 + |\varphi_+|^2 + |\varphi_-|^2} E_0, \quad (8)$$

and the refractive index change, formulated by Eq. (6-3), can be obtained by using $E = E_{sc} + E_{ext}$. Note that the externally applied electric field is spatially uniform, yielding a uniform refractive index change, which almost does not contribute to the intensity evolution and can be safely ignored. Thus the effective refractive index change has a form of

$$\Delta n = \gamma \frac{|\varphi_+|^2}{2 + |\varphi_+|^2 + |\varphi_-|^2} - \gamma \frac{|\varphi_-|^2}{2 + |\varphi_+|^2 + |\varphi_-|^2}, \quad (9)$$

where $\gamma = \frac{1}{2} n_0^3 r_{33} E_0$. Equation (9) shows a competition between self-focusing (the 1st term) and -defocusing (the 2nd term) nonlinearities. By inserting Eq. (9) into Eq. (6-1) and Eq. (6-2), one can build a time-independent model for light propagation under the stroboscopic nonlinearity.

3. Simulation of beam dynamics

In this part, we demonstrate the validity of the time-independent model by studying two reported scenarios. One is associated with the breaking of action–reaction principle in the interaction of two beams [21], and the other is related to vector solitons formed under the stroboscopic nonlinearity [23].

3.1 Breaking action–reaction principle in light interactions

Two stroboscopic Gaussian beams are employed here. One of them, synchronized with the positive external electric field, feels a self-focusing nonlinearity, while the other with the negative external electric field undergoes a self-defocusing nonlinearity. The spatial profiles of the former and the latter are $\varphi_+ = A e^{-[(x-d)/w]^2}$ and $\varphi_- = A e^{-(x/w)^2}$, respectively, where the beam spacing is $d = 9.6 \mu\text{m}$, and the amplitude and width for both beams are $A = 1.4$ and $w = 13.6 \mu\text{m}$. The propagation dynamics of the two beams, calculated using the time-independent model, are presented in Figs. 3(a, b). Both beams deflect downward owing to the breaking of action–reaction principle. For comparison, the beam dynamics are also simulated via the time-dependent model when the system reaches a quasi-steady state, as shown in Figs. 3(c, d), where the light intensity is averaged over one period. The time-independent results (I_{\pm}) are in good agreement with their time-dependent counterparts ($I_{t\pm}$). Indeed, the two cases match well in detail, as illustrated by the comparison of their intensity profiles in Figs. 3(e-h). Furthermore, we compare the empirical model ($I_{0\pm}$) [21] with the time-dependent model [Figs. 3(i-l)]. Apparent discrepancies are observed in their intensity distributions, which invalidates the precision of the empirical model.

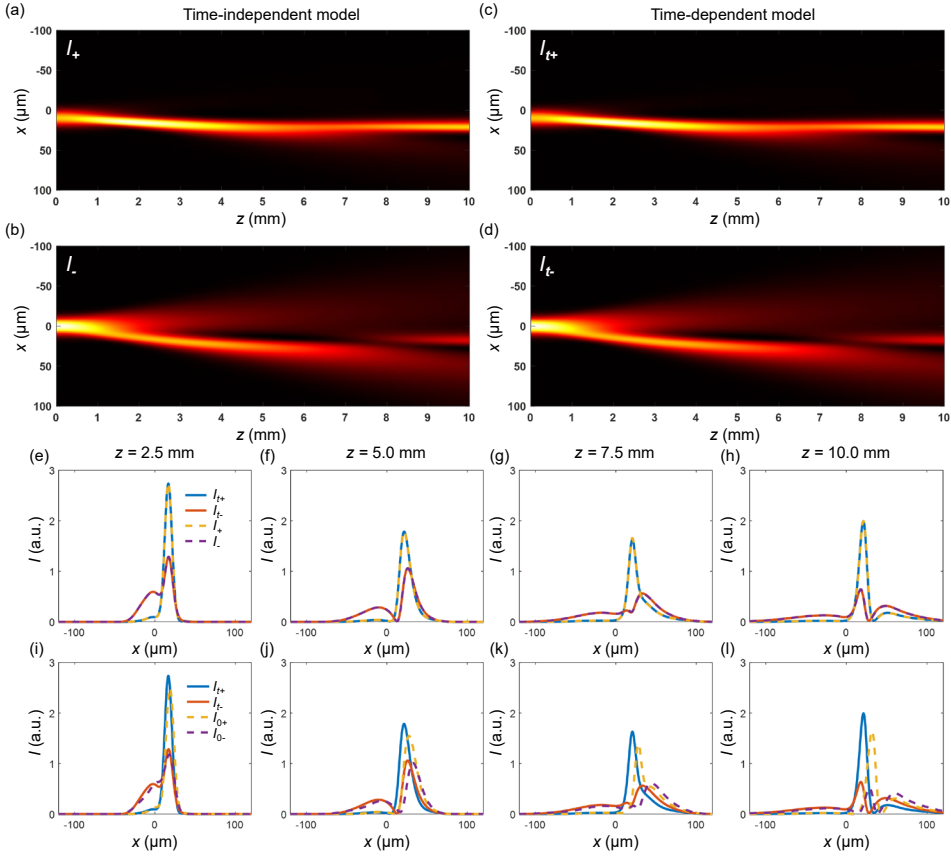


Fig. 3. Simulated interactions of two beams violating action–reaction principle using different models. (a-d) Beam propagation calculated by the time-independent (a, b) and time-dependent (c, d) models. (e-l) Beam intensity profiles at several chosen distances for the beam dynamics based on the time-independent (I_{\pm}), time-dependent ($I_{t\pm}$) and empirical models ($I_{0\pm}$).

3.2 Dynamics of a vector soliton

To obtain a vector soliton in the time-independent model, we let $\varphi_+ = u_+(x) \exp(i\beta z)$ and $\varphi_- = u_-(x) \exp(i\beta z)$, where $u_{\pm}(x)$ are real and β is an eigenvalue. Then Eqs. (6, 9) are reshaped to:

$$\frac{1}{2n_0k_0} \frac{\partial^2 u_+}{\partial x^2} - \beta u_+ + k_0 \gamma \frac{|u_+|^2 - |u_-|^2}{2 + |u_+|^2 + |u_-|^2} u_+ = 0, \quad (10-1)$$

$$\frac{1}{2n_0k_0} \frac{\partial^2 u_-}{\partial x^2} - \beta u_- + k_0 \gamma \frac{|u_+|^2 - |u_-|^2}{2 + |u_+|^2 + |u_-|^2} u_- = 0. \quad (10-2)$$

One vector soliton, as presented in the inset of Fig. 4(a), is obtained by numerically solving the above equations. Its propagation dynamics, simulated by the time-independent and -dependent models, show a high consistence, while the dynamics based on the empirical and time-dependent models exhibit significant deviations. We show these comparisons quantitatively by using the following parameter:

$$S = \frac{\int I_1(x)I_2(x)dx}{\sqrt{\int [I_1(x)]^2 dx} \sqrt{\int [I_2(x)]^2 dx}}, \quad (11)$$

which characterizes the similarity of two beam profiles (for instance, I_1 and I_2) calculated using different models. The parameter S ranges from 0 to 1, with a higher value indicating better similarity. In particular, $S = 1$ denotes an exact overlapping of the two intensity profiles. The comparison between the time-independent and -dependent models is summarized in Fig. 4(a). Note that the intensity is averaged in a period in the time-dependent case. The value of S remains nearly 1 along the propagation direction for both components of the vector soliton, indicating that the time-independent model is valid for describing the stroboscopic nonlinearity in the quasi-steady state during the soliton propagation. In contrast, the empirical model shows a distinct deviation when compared to the time-dependent model [Fig. 4(b)]. Using the parameter S , we also compare the three models for calculating the case in Section 3.1, and similar conclusions are obtained [Figs. 4(c, d)]: the time-dependent model describes the stroboscopic nonlinear dynamics well.

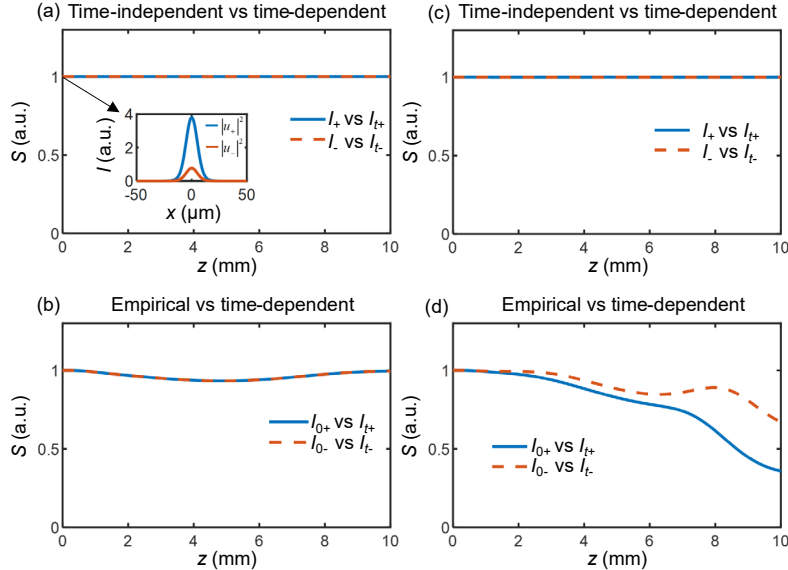


Fig. 4. Comparison of beam dynamics based on different models using the parameter S . Top row: time-independent vs time-dependent model. Bottom row: empirical vs time-dependent model. Left and right columns correspond to the dynamics of a vector soliton [see the inset in (a)] and two interacting Gaussian beams employed in Section 3.1, respectively.

4. Conclusion

In conclusion, we have revealed the underlying physical mechanism of stroboscopic nonlinear dynamics and established an effective time-independent model to describe them. We find that, when the stroboscopic period is much shorter than the dielectric time constant of the crystal, the dynamics eventually evolve into a quasi-steady state in which opposite nonlinear processes effectively coexist. This coexistence gives rise to an unconventional form of optical nonlinearity that cannot be realized in static systems. Quantitative comparisons indicate that the derived time-independent model describes the quasi-steady state of the time-dependent dynamics well, while generating more accurate calculations than the previously used empirical model. These results provide a clear and rigorous understanding of stroboscopic nonlinear

dynamics and highlight time modulation as a powerful strategy for engineering optical nonlinearities.

Funding. National Key R&D Program of China (2025YFA1411800); National Natural Science Foundation of China (NSFC) (12250009); 111 Project in China (B23045).

Disclosures. The authors declare no conflicts of interest.

Acknowledgment. We acknowledge financial support from the National Key R&D Program of China (2025YFA1411800), the National Natural Science Foundation of China (NSFC) (12250009) and the 111 Project in China (B23045).

Data availability. Data underlying the results presented in this paper are not publicly available at this time but may be obtained from the authors upon reasonable request.

References

1. B. Apffel, F. Novkoski, A. Eddi, and E. Fort, “Floating under a levitating liquid,” *Nature* **585**, 48-52 (2020).
2. A. A. Grandi, S. Protière, and A. Lazarus, “Enhancing and controlling parametric instabilities in mechanical systems,” *Extreme Mech. Lett.* **43**, 101195 (2021).
3. H. Lira, Z. Yu, S. Fan, and M. Lipson, “Electrically driven nonreciprocity induced by interband photonic transition on a silicon chip,” *Phys. Rev. Lett.* **109**, 033901 (2012).
4. S. Saha, O. Segal, C. Fruhling, E. Lustig, M. Segev, A. Boltasseva, and V. M. Shalaev, “Photonic time crystals: a materials perspective,” *Opt. Express* **31**, 8267-8273 (2023).
5. J. Zhang, P. W. Hess, A. Kyprianidis, P. Becker, A. Lee, J. Smith, G. Pagano, I.-D. Potirniche, A. C. Potter, A. Vishwanath, N. Y. Yao, and C. Monroe, “Observation of a discrete time crystal,” *Nature* **543**, 217-220 (2017).
6. J. Jiang, E. Bernhart, M. Röhrle, J. Benary, M. Beck, C. Baals, and H. Ott, “Kapitza trap for ultracold atoms,” *Phys. Rev. Lett.* **131**, 033401 (2023).
7. P. L. Kapitza, “Dynamic stability of the pendulum with vibrating suspension point,” *Sov. Phys. JETP* **21**, 588-597 (1951).
8. C. Wagner, H. W. Müller, and K. Knorr, “Faraday waves on a viscoelastic liquid,” *Phys. Rev. Lett.* **83**, 308 (1999).
9. R. Fleury, D. L. Sounas, and A. Alù, “Subwavelength ultrasonic circulator based on spatiotemporal modulation,” *Phys. Rev. B* **91**, 174306 (2015).
10. D. Sounas and A. Alù, “Non-reciprocal photonics based on time modulation,” *Nat. Photonics* **11**, 774-783 (2017).
11. A. Dikopoltsev, Y. Sharabi, M. Lyubarov, Y. Lumer, S. Tsesses, E. Lustig, I. Kaminer, and M. Segev, “Light emission by free electrons in photonic time-crystals,” *Proc. Natl. Acad. Sci. U.S.A.* **119**, e2119705119 (2022).
12. M. Lyubarov, Y. Lumer, A. Dikopoltsev, E. Lustig, Y. Sharabi, and M. Segev, “Amplified emission and lasing in photonic time crystals,” *Science* **377**, 425-428 (2022).
13. Y. Pan, M.-I. Cohen, and M. Segev, “Superluminal k-gap solitons in nonlinear photonic time crystals,” *Phys. Rev. Lett.* **130**, 233801 (2023).
14. S. Choi, J. Choi, R. Landig, G. Kucsko, H. Zhou, J. Isoya, F. Jelezko, S. Onoda, H. Sumiya, V. Khemani, C. v. Keyserlingk, N. Y. Yao, E. Demler, and M. D. Lukin, “Observation of discrete time-crystalline order in a disordered dipolar many-body system,” *Nature* **543**, 221-225 (2017).
15. B. Liu, L.-H. Zhang, Q.-F. Wang, Y. Ma, T.-Y. Han, J. Zhang, Z.-Y. Zhang, S.-Y. Shao, Q. Li, H.-C. Chen, B.-S. Shi, and D.-S. Ding, “Higher-order and fractional discrete time crystals in Floquet-driven Rydberg atoms,” *Nat. Commun.* **15**, 9730 (2024).
16. J. Smits, L. Liao, H. T. C. Stoof, and P. van der Straten, “Observation of a space-time crystal in a superfluid quantum gas,” *Phys. Rev. Lett.* **121**, 185301 (2018).
17. H. Alarcón, M. Herrera-Muñoz, N. Périnet, N. Mujica, P. Gutiérrez, and L. Gordillo, “Faraday-wave contact-line shear gradient induces streaming and tracer self-organization: From vortical to hedgehoglike patterns,” *Phys. Rev. Lett.* **125**, 254505 (2020).
18. P. Engels, C. Atherton, and M. A. Hoefer, “Observation of Faraday waves in a Bose-Einstein condensate,” *Phys. Rev. Lett.* **98**, 095301 (2007).
19. K. Kwon, K. Mukherjee, S. J. Huh, K. Kim, S. I. Mistakidis, D. K. Maity, P. G. Kevrekidis, S. Majumder, P. Schmelcher, and J.-y. Choi, “Spontaneous formation of star-shaped surface patterns in a driven Bose-Einstein condensate,” *Phys. Rev. Lett.* **127**, 113001 (2021).
20. Z. Zhang, K.-X. Yao, L. Feng, J. Hu, and C. Chin, “Pattern formation in a driven Bose-Einstein condensate,” *Nat. Phys.* **16**, 652-656 (2020).
21. W. Ma, Y. Zhuang, Z. Wang, P. Jia, P. Zhang, Y. Hu, Z. Chen, and J. Xu, “Breaking the action-reaction principle of light interactions under a stroboscopic nonlinearity,” *Laser Photonics Rev.* **17**, 2200177 (2023).

22. J. Wu, Y.-H. Zhuang, Y. Hu, and J.-J. Xu, “Optical spiral predator–prey dynamics,” *Chin. Phys. Lett.* **42**, 024202 (2025).
23. Y.-H. Zhuang, J. Wu, S.-Y. Li, Y. Hu, Z.-G. Chen, and J.-J. Xu, “Unusual impulse–momentum relationship in non-reciprocal light interactions,” *Light: Sci. Appl.* (2026), in press.
24. B. Crosignani, P. Di Porto, A. Degasperis, M. Segev, and S. Trillo, “Three-dimensional optical beam propagation and solitons in photorefractive crystals,” *J. Opt. Soc. Am. B* **14**, 3078–3090 (1997).
25. C. Dari-Salisburgo, E. DelRe, and E. Palange, “Molding and stretched evolution of optical solitons in cumulative nonlinearities,” *Phys. Rev. Lett.* **91**, 263903 (2003).
26. E. DelRe, B. Crosignani, and P. Di Porto, “Photorefractive solitons and their underlying nonlocal physics,” *Prog. Opt.* **53**, 153–200 (2009).
27. W. Horn, J. v Bassewitz, and C. Denz, “Slow and fast light in photorefractive SBN: 60,” *J. Opt.* **12**, 104011 (2010).
28. E. Beyreuther, J. Ratzenberger, M. Roeper, B. Kirbus, M. Rüsing, L. I. Ivleva, and L. M. Eng, “Photoconduction of polar and nonpolar cuts of undoped $\text{Sr}_{0.61}\text{Ba}_{0.39}\text{Nb}_2\text{O}_6$ single crystals,” *Crystals* **11**, 780 (2021).